Pizarro, F., Sánchez-Cabello, C., Vazquez-Roy, J.-L., & Rajo-Iglesias, E. (2020). Considerations of impedance sensitivity and losses in designing inverted microstrip gap waveguides. *In AEU - International Journal of Electronics and Communications, 124*, 153353-153359

DOI:10.1016/j.aeue.2020.153353

Considerations of impedance sensitivity and losses in designing inverted microstrip gap waveguides

Francisco Pizarro[a,*], Carlos Sánchez-Cabello[b], Jose-Luis Vazquez-Roy[b] and Eva Rajo-Iglesias[b]

[a]Pontificia Universidad Católica de Valparaíso, Escuela de Ingeniería Eléctrica, Valparaíso
[b]Department of Communications and Signal Theory, Universidad Carlos III de Madrid, 28911 Madrid, Spain

ARTICLE INFO

Keywords:
gap waveguide technology
parallel plate mode
artificial magnetic conductor

ABSTRACT

One of the versions of gap waveguide technology, the inverted microstrip, is studied in terms of the effects that the parameters of the substrate and the bed of nails used for its implementation have in the behaviour as a transmission line. Mainly, the line impedance sensitivity and the losses are evaluated for different design parameters. To this aim, a methodology based on simulations is described and some experimental verifications are as well included. The results are of great interest for designers of antennas and components in this technology.

1. Introduction

Gap waveguide technology was first proposed in 2009 [1] and demonstrated in 2011 [2]. Since then, the technology has advanced in all its different implementations such as the ridge [3], groove and inverted microstrip (also known as suspended microstrip [4]) gap waveguides. Inverted microstrip gap waveguide topology has larger losses than the groove and ridge versions [5], [6], but it has advantages from the point of view of simplicity of design and manufacturing. A description of the waveguide is presented in Fig. 1. The design simplicity is due to the fact that in this version the periodic structure (bed of nails) is uniform and the circuit design is made in a similar way as for conventional inverted microstrip technology. With respect to the manufacturing, the circuit is made with standard PCB manufacturing techniques and a uniform bed of nails is used as an Artificial Magnetic Conductor (AMC). As consequence, this topology is a good candidate in terms of compromise solution between losses and complexity [7] for the design of complicated circuits such as high-order filters, diplexers, or feed networks. Recently, their losses have been measured at 60 GHz [8], showing how this technology outperforms any alternative printed technology, and designs in this technology up to that frequency band have been presented such as filters [9] and feed networks [10].

Even if designs made with inverted microstrip gap waveguide technology have been presented, there is still an unsolved important aspect to be considered when facing a new design: how to choose the dimensions of the bed of nails and the thickness of the substrate. No studies that explain how the relative position within the stop-band (related with the selected pin's height) or any of the other parameters affect the losses exist.

These two parameters can definitely affect the performance of the circuit. On the one hand, and in an ideal case, the bed of nails should provide the perfect magnetic conductor (PMC) condition in an homogeneous way in order to make the placement of the different lines or discontinuities of the circuit under design independent of the relative position of the bed of nails (BoN). However, it has been reported in previous works [11] how the sensitivity of the line impedance with respect to this position is not always negligible. On the other hand, moving up in frequency implies the use of very thin substrates that may experience deformations. Obviously, this affects the gap size and consequently the local impedance. How much this substrate thickness affects the performance in terms of impedance sensitivity and losses is another key aspect to be treated in this work.

The calculation of the line impedance in this particular version of the gap waveguide has deserved a lot of attention from the beginning of the use of the technology [4]. As there is a periodic structure involved in this calculation, the impedance differs from the one in a regular inverted microstrip line. Different options have been considered to calculate

*This work has been funded by FONDECYT INICIACION 11180434, CONICYT PCI MEC80180108, and the Spanish Ministry of Economy under project TEC2016-79700-C2-2-R.
*Corresponding author
francisco.pizarro.t@pucv.cl (F. Pizarro); dramirez@tsc.uc3m.es (C. Sánchez-Cabello); jvazquez@tsc.uc3m.es (J. Vazquez-Roy); eva@tsc.uc3m.es (E. Rajo-Iglesias)
ORCID(s):

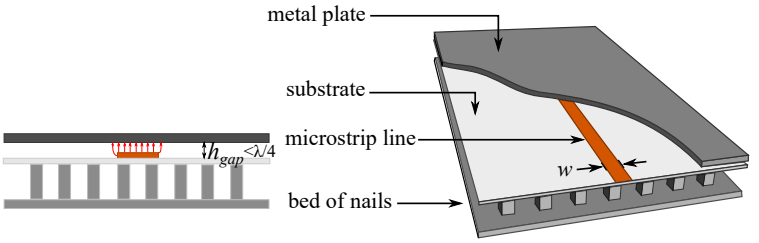

Figure 1: Description of inverted microstrip gap waveguide technology.

the value of this impedance, from the one proposed in [12] to a more accurate one developed in [11]. More recently, analytical methods have been proposed [13] to this aim and also the calculation of the impedance for the ridge version of this technology was recently revisited [14], meaning that this is an issue that still is of interest.

Parametric studies are of great importance for the design of any high frequency circuit, in order to improve the performances of future designs [15, 16, 17]. Under this scope, the purpose of this work is to analyse the sensitivity of the line impedance variation with the position and the losses of the line mainly as a function of the dielectric thickness, periodicity of the BoN and the position of the operation frequency with respect to the stop-band created by the pins (at the beginning, in the middle or at the end of the stop-band). We will consider the Ka-band to conduct this analysis, which is a candidate band for the future generation of communications 5G. Section II presents the studies about the impedance of the line, together with the methodology used for the calculations whilst the analysis of the losses is presented in Section III based on the study of the S_{21} parameter in a two-port network configuration. The conclusions will be validated with some experimental results presented in Section IV and the main conclusions will be summarized in Section V.

2. Study of the line impedance

By using different techniques to compute the impedance, a sensitivity analysis with respect to the different parameters of design has been presented in [18]. One of the main derived conclusions is that the key aspect to have a minor sensitivity in the impedance is the periodicity of the BoN. The denser the bed of pins is, the smaller the variation of the impedance will be or in other words, the closer to a uniform PMC behaviour will be.

A periodically loaded transmission line can be described by means of its Bloch impedance. In what follows, the characteristic impedance of an equivalent smooth transmission line will be used instead for the study. The ABCD parameters of a two-port network consisting on the transmission line containing N rows of the bed of nails and excited with conventional waveguide ports are calculated first. Since an ideal lossless transmission line with length l, characteristic impedance Z_0 and propagation constant $\gamma = j\beta$, has an ABCD matrix given by eq. (1):

$$\begin{pmatrix} A & B \\ C & D \end{pmatrix} = \begin{pmatrix} \cos\beta l & jZ_0 \sin\beta l \\ jY_0 \sin\beta l & \cos\beta l \end{pmatrix} \tag{1}$$

then, for the reciprocal and symmetrical case it is straightforward to obtain an estimation of the characteristic impedance:

$$Z_0 = \sqrt{\frac{B}{C}} \tag{2}$$

Then the procedure described in [19] can be used, where a second two-port network with $N-1$ periods is cascaded to original one with the aim of reducing the size to that of one unit cell and to avoid the numerical instabilities related to the branch selection for the solution of the complex square root in (2). A similar methodology was employed in [20] for calculating the dispersion diagram of lossy guiding structures.

In Fig. 2 the results of the impedance relative error (IRE) with respect to the PMC ideal case ($IRE(\%) = (Z_{pin} - Z_{PMC})/Z_{PMC} * 100$) from the previous proposed method at 30 GHz for $N = 6$ as function of the pin height are shown. Two relative line position cases shown in Fig. 3 (the microstrip line placed in between two rows of pins and the microstrip line placed over the pins) are considered. In addition, the results were calculated for three typical line

impedances with their corresponding line widths w: 35 Ω (w = 3.61 mm), 50 Ω (w = 2.18 mm) and 70 Ω (w = 1.24 mm). Also, two different substrate heights (h_s = 0.508 mm and h_s = 0.762 mm) and two pin periods (p = 2.5 mm and p = 1.6 mm) were used. In all cases the width of the pins was 0.8 mm, the gap 0.508 mm and the substrate a lossless Rogers RO4003. For all the simulations, an inverted microstrip line with an ideal PMC case was used as reference. Regarding the simulation setup, CST Waveguide ports were used for the excitation of the different structures used in this study. Given that the port size has an important impact on the simulated response, a study was carried out for the 50 Ω case to establish the value for the port width that gives a good estimation with the extraction method described, trying to keep its size as small as possible. Ideal PMC and PEC boundary conditions were used for this purpose. A port width w_p of four times the strip width w was found to be enough to get very accurate results. Besides, in all the BoN simulated cases, the waveguide port was extended vertically to cover half of the pin's height to ensure a quasi-TEM excitation between the PEC and the microstrip line. That is to say, the height of the port h_p is equal to half the size of the pins, plus the substrate height and the gap size. A representation of the waveport characteristics is shown in Figure 3.

The anomalous behavior of some of the curves for small pin heights is due to the proximity of the operation frequency to the lower limit of the BoN stop-band (the stop-bands for each of the selected cases are shown in Fig. 4.) From the results obtained with these simulations, the following conclusions can be derived:

- The relative error of the line impedance using a BoN in comparison with the PMC case is always higher when the pins height increases (the increase in the pin height moves the stop band down in frequency [21]). This means that if the initial design is made using the ideal PMC condition, when selecting the BoN to emulate the PMC, if the operation frequency is located at the beginning of the stopband, the behavior of the lines in terms of impedance will be closer to the ideal case.
- For the nominal substrate height (h_s = 0.508 mm), the impedance variation with respect to the position of the line is higher when the line is located between two rows of pins, except for w = 3.61 mm, where the variation is higher when the line is over a row pins.
- The obtained impedance is smaller than the reference value in all the cases but w = 3.61 mm (wide line) for the smallest pin heights.
- For higher substrate thickness, a lower variation of the impedance regarding the pin height is observed.
- For the shorter period case (p = 1.6 mm) the difference between the two line positions cases is lower.
- The impedance variations of the studied cases are moderate in all cases in terms of their effect on return losses for the terminated two-port network.

3. Losses analysis

Another key aspect to be considered is the effect of the same considered parameters in terms of losses. To this aim, simulations based on resonators were carried out in the past [5]. When the frequency under study is high enough, another option to analyze the losses is by using a long line (of at least 10λ) to calculate the α as in [8] and [6]. This is the methodology used in this work.

Here again, the objective is to assess the effect of the position of the selected operation frequency within the stop-band provided by the pins and the influence of other parameters over the losses of the topology. The same parameters as in Section II will be considered.

A 50 Ω printed line of width 2.18 mm and length 10 cm is etched on a Rogers RO4003 (ε_r=3.55, tanδ=0.0027). Two thicknesses of the substrate h_{sub} are used: 0.508 and 1.016 mm. The gap and pin width are the same as before, i.e., 0.508 mm and 0.8 mm, while the pin periodicity p varies from 1.6 to 2.5 mm and the pin height h_{pin} takes discrete values of 1.5, 2.0 and 2.8 mm. The shown studied cases for simulations are a combination of the following variations:

- Variation of h_{pin} with values of 2.8, 2.0 an 1.5 mm.
- Variation of h_{sub} with values of 0.508 mm and 1.016 mm (named “thick" case).

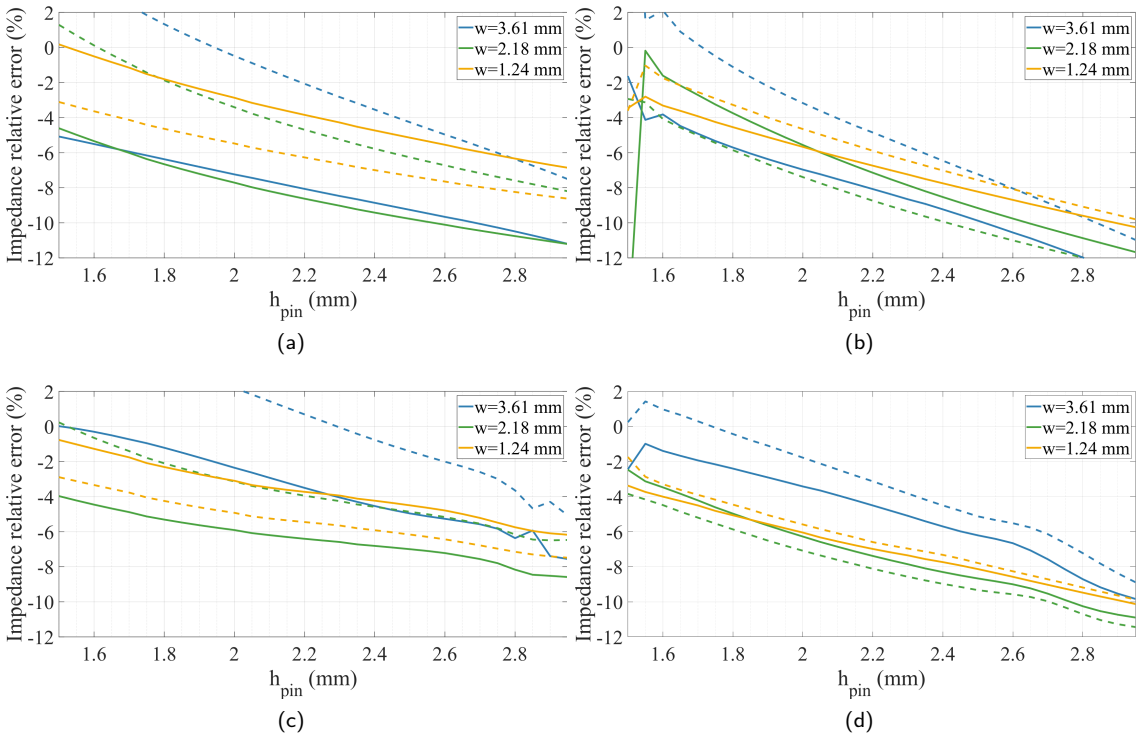

Figure 2: Simulated impedance relative error with respect to the ideal PMC case, at 30 GHz, as a function h_{pin} for two reference positions of the line with respect the pins: over the pin (dashed lines) and between two pins (solid lines) and for different substrate heights and pin periods. a) h_s=0.508 mm and p=2.5 mm. b) h_s=0.508 mm and p=1.6 mm. c) h_s=0.762 mm and p=2.5 mm. d) h_s=0.762 mm and p=1.6 mm.

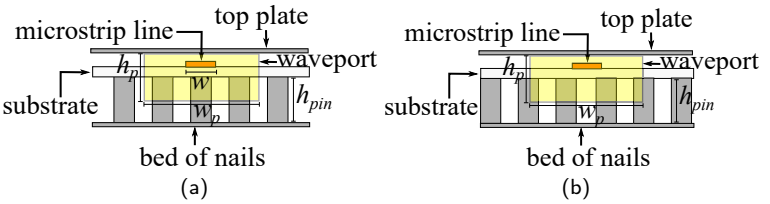

Figure 3: Inverted microstrip line position with respect to the pins and port excitation characteristics. a) Over a row of pins. b) In between two rows of pins.

- Variation of p with values of 2.5 and 1.6 mm.
- Variation of line position with respect the pins: in between pins and over a pin (named “shift" case).
- Pins made of perfect conductor (PEC) and made with a finite conductivity material such as aluminium of $\sigma = 3.77 \times 10^7$ S/m (named “lossy" case)

The named “nominal" case is now the inverted microstrip line with $h_{sub} = 0.508$ mm, pins made of PEC and the line placed in between two rows of pins (Fig. 3.b).

A summary of the simulated results is presented in Fig. 5, that shows transmission coefficient $|S_{21}|$ of the inverted microstrip gap waveguide as a function of the frequency and for the studied cases previously described. From the simulation results we can see that for all the proposed scenarios, the transmission losses are lower on the thinner substrate cases. In addition, the position of the microstrip line with respect the pins has a small influence on the

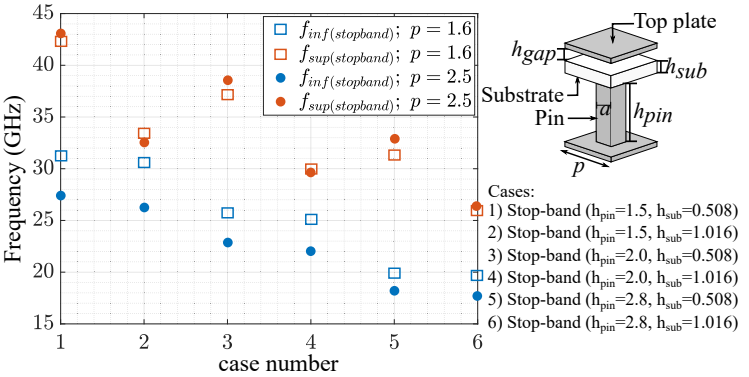

Figure 4: Lower and upper bounds of the stop-bands for the different simulated cases as a function of its parameters. All dimensions are in mm

behavior of the transmission coefficient, i.e., on the losses. The pin height, as it has an influence on the stop-band frequencies, will change the behavior of the transmission line specially when the operation frequency is close to the lower frequency limit of the stop band created by the pins (best behaviour) but not as evident as for the case of the impedance. The periodicity also has an influence over the band, but does not add any additional losses on the line. Finally, if the pins have a finite conductivity, the transmission losses are slightly higher.

4. Experimental results

Taking into account the results in Fig. 5 two pin structures have been selected to be constructed which corresponds to a bed of nails of $h_{pin} = 2.8$ mm and a bed of nails of $h_{pin} = 2.0$ mm, having both the same period between pins of $p = 2.5$ mm. In addition, the two substrate thicknesses previously studied have been used for etching the transmission lines (Rogers RO4003 with heights of 0.508 and 1.16 mm). In order to ensure a constant gap size, an Evonik foam of 0.5 mm was used between the substrate and the top metal plate. Fig. 6 shows the manufactured inverted microstrip gap waveguide.

The manufactured structures are fed with a contact 50Ω transition from a conventional microstrip line made in a substrate with the thickness of the gap and overlapping the two of them as shown in Fig. 6. At the end of each transition, a 50Ω Southwest 1092-04A-5 end-launch connector was used. To remove the effect of this end-launch connector and a TRL calibration kit was designed and manufactured.

The transmission coefficients of the mounted structures were measured using an ANRITSU MS46122B Vector Network Analyzer. The measured results for the two periodic structures and two different substrate heights are presented in Fig. 7. In order to evaluate only the transmission losses introduced by the structure we have removed the influence of the input reflection in S_{11}. In the figure, the sign f_{band} indicates the theoretical upper bound frequency of the stop-band for the corresponding measured case (taken from Fig. 4), which corresponds to case 4 ($h_{pin} = 2.0$ mm, h_{sub} =1.016 mm and $p = 2.5$ mm) and case 6 ($h_{pin} = 2.8$ mm, h_{sub} =1.016 mm and $p = 2.5$ mm). As expected, the cases with the thicker substrate have higher losses, and this become more important while increasing the frequency on the band. Concerning the variations of the pin height, the measurement results confirm the results from simulations.

5. Conclusion

In this work, an analysis of the effect on the line impedance and losses as function of several parameters of an inverted microstrip gap waveguide structure was presented. The parameters included variations of the dielectric and the bed of nails characteristics and the variation of the line impedance with the relative position of it with respect to the pins and for the first time for different pins heights has been evaluated. There is a clear influence of these two parameters on the line impedance. A thicker dielectric reduces the variation of the impedance in all cases and the impedance is closer to the one calculated using an ideal PMC when the frequency of use is close to the beginning of the stop band.

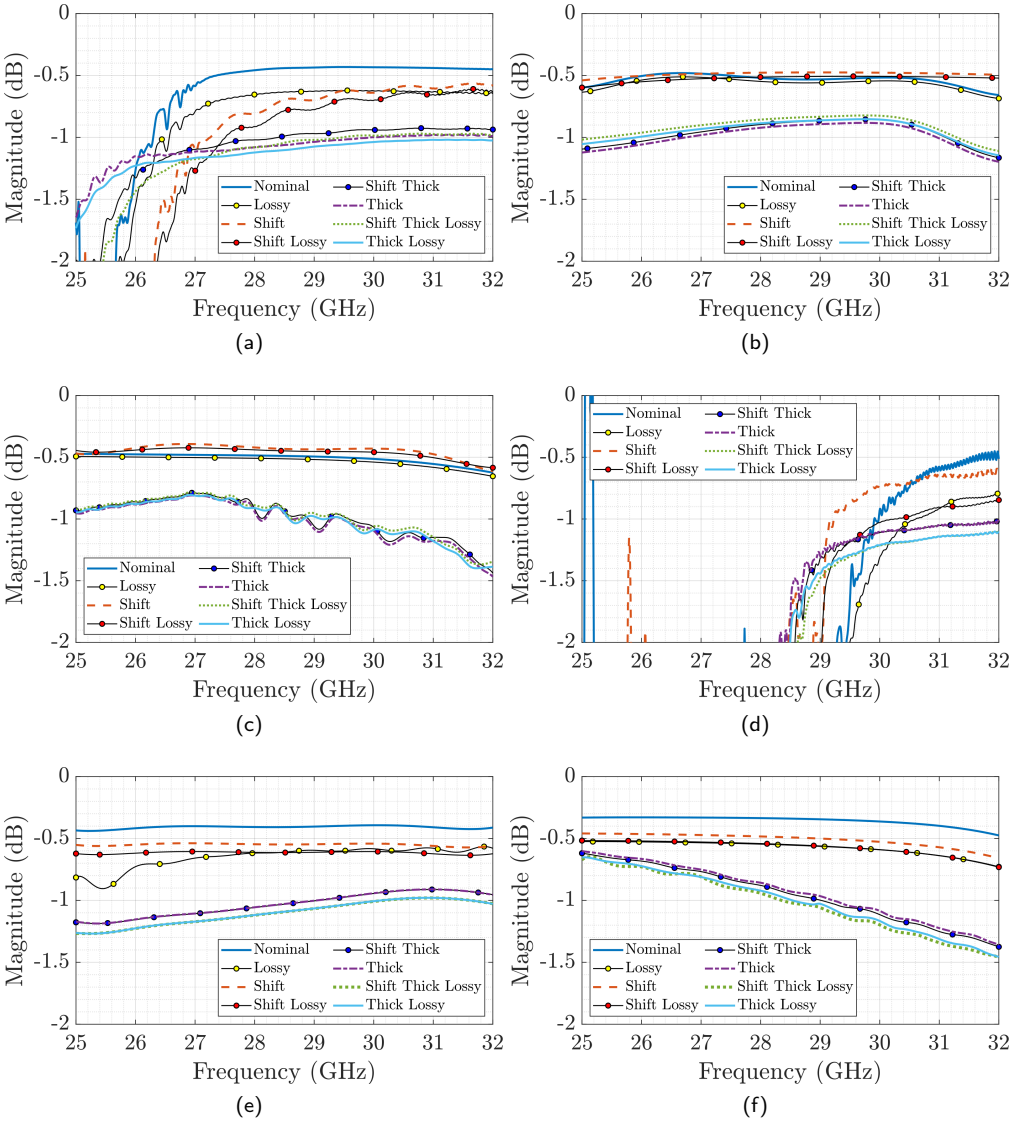

Figure 5: Simulated $|S_{21}|$ as function of the frequency for different inverted microstrip gap waveguide. a) $h_{pin} = 1.5$ mm, $p = 2.5$ mm b) $h_{pin} = 2.0$ mm, $p = 2.5$ mm c) $h_{pin} = 2.8$ mm, $p = 2.5$ mm d) $h_{pin} = 1.5$ mm, $p = 1.6$ mm. e) $h_{pin} = 2.0$ mm, $p = 1.6$ mm f) $h_{pin} = 2.8$ mm, $p = 1.6$ mm.

The line losses have been evaluated using a long line (10λ). The parameter that affects more the losses is the dielectric thickness while the relative position of the line with respect to the pins has a negligible effect on the losses.

Acknowledgment

The authors would like to thank professor Luis Fernando Herran, from the Universidad de Oviedo, for the construction of the TRL calibration kit and the microstrip transitions.

References

[1] P.-S Kildal, E. Alfonso, A. Valero-Nogueira, and E. Rajo-Iglesias. Local metamaterial-based waveguides in gaps between parallel metal plates. *IEEE Antennas and Wireless Propagation Letters*, 8:84–87, 2009.

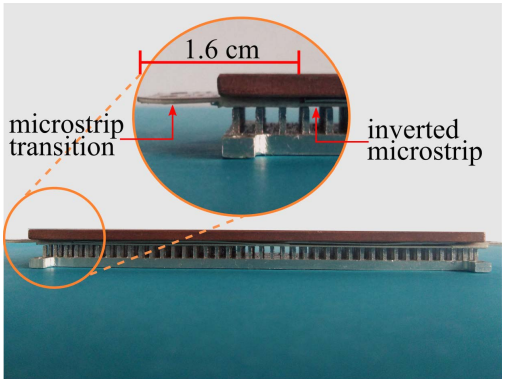

Figure 6: Manufactured inverted microstrip gap waveguide with 50 Ω microstrip line transition

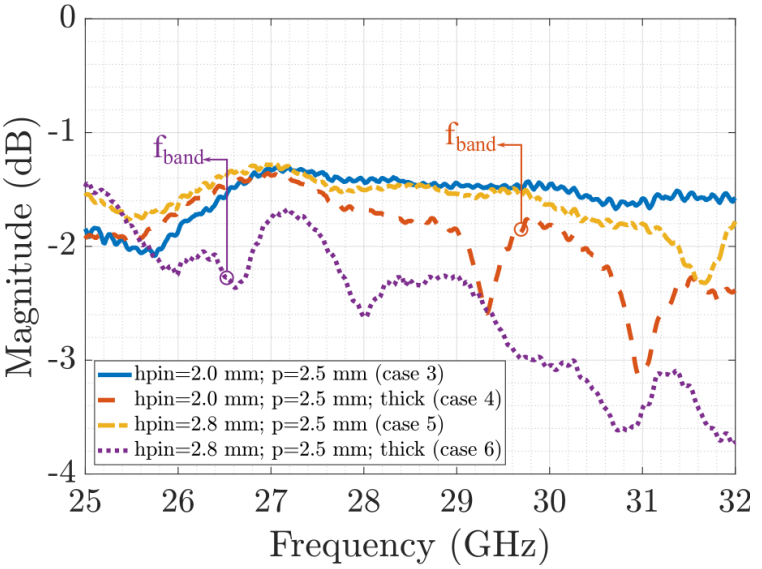

Figure 7: Measured transmission coefficients as a function of the frequency for the manufactured inverted microstrip gap waveguides referred to the cases depicted in Figure 4.

[2] P.-S. Kildal, A.U. Zaman, E. Rajo-Iglesias, E. Alfonso, and A. Valero-Nogueira. Design and experimental verification of ridge gap waveguide in bed of nails for parallel-plate mode suppression. *IET Microwaves, Antennas and Propagation*, 5(3):262 –270, 21 2011. ISSN 1751-8725. doi: 10.1049/iet-map.2010.0089.

[3] Efat Nematpour, Mohamad Hossein Ostovarzadeh, and Seyed Ali Razavi. Development of a wide band TEM-based Bethe hole coupler using ridge gap waveguide technology. *AEU - International Journal of Electronics and Communications*, 111:152933, 2019. ISSN 1434-8411. doi: https://doi.org/10.1016/j.aeue.2019.152933. URL http://www.sciencedirect.com/science/article/pii/S1434841119315791.

[4] A. Valero-Nogueira, M. Baquero, J.I. Herranz, J. Domenech, E. Alfonso, and A. Vila. Gap waveguides using a suspended strip on a bed of nails. *IEEE Antennas and Wireless Propagation Letters,*, 10:1006–1009, 2011. ISSN 1536-1225. doi: 10.1109/LAWP.2011.2167591.

[5] E. Pucci, A. U. Zaman, E. Rajo-Iglesias, P. S. Kildal, and A. Kishk. Study of Q-factors of ridge and groove gap waveguide resonators. *IET Microwaves, Antennas and Propagation*, 7(11):900–908, August 2013. ISSN 1751-8725. doi: 10.1049/iet-map.2013.0081.

[6] E. Rajo-Iglesias, M. Ferrando-Rocher, and A. U. Zaman. Gap waveguide technology for millimeter-wave antenna systems. *IEEE Communications Magazine*, 56(7):14–20, July 2018. ISSN 0163-6804. doi: 10.1109/MCOM.2018.1700998.

[7] E. Pucci, E. Rajo-Iglesias, J. L. Vazquez-Roy, and P. S. Kildal. Planar dual-mode horn array with corporate-feed network in inverted microstrip gap waveguide. *IEEE Transactions on Antennas and Propagation*, 62(7):3534–3542, July 2014. ISSN 0018-926X. doi: 10.1109/TAP.2014.2317496.

[8] A.A. Brazalez, E. Rajo-Iglesias, J.-L. Vazquez-Roy, A. Vosoogh, and P.-S. Kildal. Design and validation of microstrip gap waveguides and their transitions to rectangular waveguide, for millimeter-wave applications. *IEEE Transactions on Microwave Theory and Techniques,*, 63 (12):4035–4050, Dec 2015. ISSN 0018-9480. doi: 10.1109/TMTT.2015.2495141.

[9] A. Vosoogh, A. A. Brazález, and P. Kildal. A v-band inverted microstrip gap waveguide end-coupled bandpass filter. *IEEE Microwave and*

Wireless Components Letters, 26(4):261–263, April 2016. ISSN 1531-1309. doi: 10.1109/LMWC.2016.2538598.

[10] J. Liu, A. Vosoogh, A. U. Zaman, and J. Yang. Design and fabrication of a high-gain 60-GHz cavity-backed slot antenna array fed by inverted microstrip gap waveguide. *IEEE Transactions on Antennas and Propagation*, 65(4):2117–2122, April 2017. doi: 10.1109/TAP.2017.2670509.

[11] A. Berenguer, M. Baquero-Escudero, D. Sanchez-Escuderos, and F. Vico. Rigorous method for calculating gap waveguides impedance using transmission line theory. In *Antennas and Propagation (EuCAP), 2014 8th European Conference on*, pages 2508–2512, April 2014. doi: 10.1109/EuCAP.2014.6902328.

[12] H. Raza, J. Yang, and P. S. Kildal. Study of the characteristic impedance of gap waveguide microstrip line realized with square metal pins. In *Antennas and Propagation (EuCAP), 2013 7th European Conference on*, pages 3001–3005, April 2013.

[13] J. Liu, J. Yang, and A. U. Zaman. Analytical solutions to characteristic impedance and losses of inverted microstrip gap waveguide based on variational method. *IEEE Transactions on Antennas and Propagation*, 66(12):7049–7057, Dec 2018. doi: 10.1109/TAP.2018.2869204.

[14] A. T. Hassan, M. A. Moharram Hassan, and A. A. Kishk. Modeling and design empirical formulas of microstrip ridge gap waveguide. *IEEE Access*, 6:51002–51010, 2018. ISSN 2169-3536. doi: 10.1109/ACCESS.2018.2869718.

[15] Ahmet Serdar Turk and Okan Mert Yucedag. Parametric analysis of flare edge rolling throat bending and asymmetric flare effects for h-plane horn radiator. *AEU - International Journal of Electronics and Communications*, 66(4):297 – 304, 2012. ISSN 1434-8411. doi: https://doi.org/10.1016/j.aeue.2011.08.006. URL http://www.sciencedirect.com/science/article/pii/S143484111100210X.

[16] Noha A. Al-Shalaby and Shaymaa M. Gaber. Parametric study on effect of solar-cell position on the performance of transparent dra transmitarray. *AEU - International Journal of Electronics and Communications*, 70(4):436 – 441, 2016. ISSN 1434-8411. doi: https://doi.org/10.1016/j.aeue.2016.01.006. URL http://www.sciencedirect.com/science/article/pii/S1434841116300061.

[17] Amir Firouzfar, Majid Afsahi, and Ali A. Orouji. Novel, straightforward procedure to design square loop frequency selective surfaces based on equivalent circuit model. *AEU - International Journal of Electronics and Communications*, 119:153164, 2020. ISSN 1434-8411. doi: https://doi.org/10.1016/j.aeue.2020.153164. URL http://www.sciencedirect.com/science/article/pii/S1434841119315043.

[18] A. Berenguer, M. Baquero-Escudero, D. Sanchez-Escuderos, and F. Vico. Reduction of the impedance dependence on the suspended-strip gap waveguide. In *Radio Science Meeting (Joint with AP-S Symposium), 2014 USNC-URSI*, pages 151–151, July 2014. doi: 10.1109/USNC-URSI.2014.6955533.

[19] A.M. Mangan, S.P. Voinigescu, Ming-Ta Yang, and M. Tazlauanu. De-embedding transmission line measurements for accurate modeling of IC designs. *EEE Transactions on Electron Devices*, 53(2):235 – 241, February 2006. ISSN 0018-9383. doi: 10.1109/TED.2005.861726.

[20] Francisco Mesa, Raúl Rodríguez-Berral, and Francisco Medina. On the computation of the dispersion diagram of symmetric one-dimensionally periodic structures. *Symmetry*, 10(8), 2018. ISSN 2073-8994. doi: 10.3390/sym10080307. URL http://www.mdpi.com/2073-8994/10/8/307.

[21] E. Rajo-Iglesias and P.-S. Kildal. Numerical studies of bandwidth of parallel-plate cut-off realised by a bed of nails, corrugations and mushroom-type electromagnetic bandgap for use in gap waveguides. *IET Microwaves, Antennas and Propagation*, 5(3):282 –289, 21 2011. ISSN 1751-8725. doi: 10.1049/iet-map.2010.0073.